

## Radially self-accelerating optical pulses

Marco Ornigotti<sup>1,2,\*</sup> and Alexander Szameit<sup>1</sup>

<sup>1</sup>*Institut für Physik, Universität Rostock, Albert-Einstein-Straße 23, 18059 Rostock, Germany*

<sup>2</sup>*Photonics Laboratory, Physics Unit, Tampere University, P.O. Box 692, FI-33101 Tampere, Finland*



(Received 28 November 2018; published 28 February 2019)

We generalize the concept of radially self-accelerating beams to the domain of optical pulses. In particular, we show how radially self-accelerating optical pulses (RSAPs) can be constructed by suitable superpositions of X-waves, which are a natural extension of Bessel beams in the pulsed domain. Moreover, we show that while field-rotating RSAPs preserve their self-acceleration character, intensity-rotating RSAPs only possess pseudo-self-acceleration, as their transverse intensity distribution is deformed during propagation due to their propagation-dependent angular velocity.

DOI: [10.1103/PhysRevA.99.023859](https://doi.org/10.1103/PhysRevA.99.023859)

### I. INTRODUCTION

In recent years, accelerating electromagnetic fields, i.e., solutions of Maxwell's equation, which propagate along curved trajectories in free space without being subject to an external force, have been the subject of rather intensive research. The archetype of an accelerating beam is surely the Airy beam, first introduced in quantum mechanics by Berry and Balazs in 1974 [1], and then brought to optics by Siviloglou and co-workers in 2007 [2,3]. Due to their exotic nature and novel features, Airy beams were studied within the context of nonlinear optics [4], particle manipulation [5], and they gave rise to very interesting and innovative applications, such as the generation of curved plasma channels [6]. Since 2007, accelerating beams were studied in different coordinate systems [7,8], and their trajectory was suitably engineered to match different forms of curved [9–11] and arbitrary [12] paths, and to find new schemes of acceleration, such as radial [13,14] and angular [15,16] accelerating beams. The former, in particular, are often referred to as radially self-accelerating beams (RSABs), and they propagate along spiraling trajectories around their optical axis due to radial acceleration.

RSABs are typically described, in the monochromatic regime, in terms of superpositions of Bessel beams, with an angular velocity proportional to the amount of orbital angular momentum they carry [13]. The distinguishing characteristic of RSABs, however, is a transverse intensity distribution that rotates around the propagation axis without exhibiting diffraction, a consequence of RSABs being represented as a sum of nondiffracting beams. RSABs, moreover, have potential applications in different areas of physics, such as sensing [6], material processing [17,18], and particle manipulation [19,20]. Despite this broad interest, however, RSABs have so far only been studied within the monochromatic regime, and the possibility of extending their properties to the domain of optical pulses has not been investigated yet. Having at hand radially self-accelerating pulses, in fact, could drastically

benefit their applications in material processing or particle manipulation, to name a few.

In this work, we focus on a generalization of the concept of self-acceleration to the pulsed domain. In doing that, we will show how it is possible to create radially self-accelerating pulses (RSAPs) using superpositions of X-waves rather than Bessel beams. This simple extension of the definition of RSAB given in Ref. [13], however, has some important consequences on the nature of the self-accelerating character of such pulses.

This work is organized as follows: In Sec. II, we briefly recall the properties and definition of RSABs. Then, in Sec. III, we show that RSAPs can be constructed by suitably generalizing their definition in the monochromatic domain as a superposition of X-waves rather than Bessel beams for both field-rotating and intensity-rotating RSAPs. For the latter case, we show that the only possible analytical form of intensity-rotating RSAPs can be obtained by assigning a different propagation constant to each monochromatic beam composing the pulse. Finally, conclusions are drawn in Sec. IV.

### II. RADIALLY SELF-ACCELERATING BEAMS

As a starting point of our analysis, let us consider a scalar monochromatic beam solution of the free-space Helmholtz equation,

$$(\nabla^2 + k^2)\psi(\mathbf{r}; k) = 0, \quad (1)$$

where  $k = 2\pi/\lambda$  is the vacuum wave vector of the beam, and  $\lambda$  is its wavelength. In cylindrical coordinates, the most general solution to the above equation can be written in terms of Bessel beams as follows:

$$\psi(\mathbf{r}; k) = \sum_m \int d\kappa A_m(\kappa) J_m(R\sqrt{k^2 - \kappa^2}) e^{im\theta + \kappa z}, \quad (2)$$

where  $J_m(x)$  is the Bessel function of the first kind [21], and the integration variable  $\kappa \propto \cos \vartheta_0$  represents the characteristic Bessel cone angle [22]. Following the prescriptions of Ref. [13], is it possible to extract RSABs from the above equation by choosing  $A_m(\kappa) = C_m \delta(\kappa - (m\Omega + \beta))$ , where

\*marco.ornigotti@uni-rostock.de

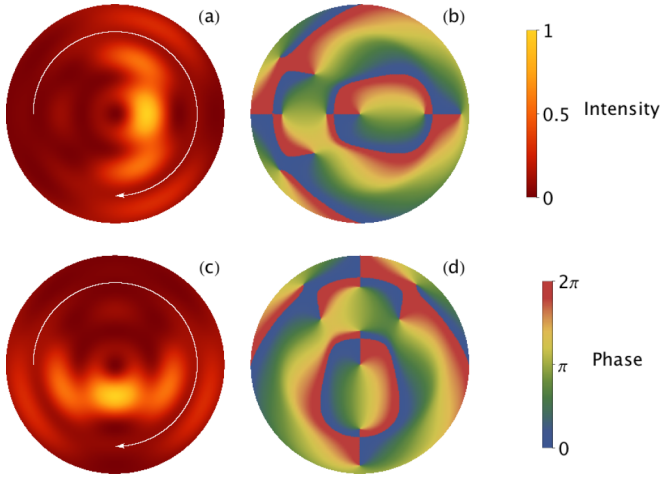


FIG. 1. Intensity and phase distribution for field rotating RSABs. Panels (a) and (c) correspond to the intensity distributions at  $z = 0$  and  $z = \pi/2\Omega$ , respectively, while panels (b) and (d) depict the correspondent phase profiles. The intensity and phase distributions have been plotted in the region  $0 < R < 12 \mu\text{m}$ . For these figures,  $\Omega = 75 \text{ rad/s}$ ,  $\lambda = 800 \text{ nm}$ ,  $\beta = 0$ , and  $C_m = 1$  for  $0 < m \leq 4$ , and  $C_m = 0$  otherwise, have been used. The white arrow in the intensity distribution shows the direction of rotation of the RSAB.

$\Omega$  is the actual angular velocity of the RSAB, and  $\beta$  is a free parameter, with the dimension of a propagation constant. This choice ensures the possibility of defining a corotating reference frame  $\Phi = \theta + \Omega z$ , in which the RSAB appears propagation-invariant, namely  $\partial\psi_{\text{RSAB}}(\mathbf{r}; k)/\partial z = 0$ . The explicit form of a RSAB thus reads

$$\psi_{\text{RSAB}}(R, \Phi; k) = e^{i\beta z} \sum_{m \in \mathcal{M}} C_m J_m(\alpha_m R) e^{im\Phi}, \quad (3)$$

where  $\alpha_m = \sqrt{k^2 - (m\Omega + \beta)^2}$  represents the transverse wave vector of the single Bessel component of the RSAB, and  $\mathcal{M} = \{m \in \mathbb{N} : \alpha_m > 0\}$ . For  $\beta = 0$ , the above equation represents the so-called field-rotating RSABs, for which both amplitude and phase spiral around the propagation direction synchronously. For  $\beta \neq 0$ , instead, Eq. (3) describes the intensity-rotating RSABs, where the amplitude and phase distributions are not synchronized anymore during their rotation along the propagation direction, although the intensity distribution remains propagation-invariant. Examples of field-rotating and intensity-rotating RSABs are given in Figs. 1 and 2, respectively.

### III. EXTENSION TO PULSE DOMAIN

To extend the concept of RSABs to the polychromatic domain, we first notice that given a solution  $\psi(\mathbf{r}; k)$  of the Helmholtz equation (1), it is possible to construct an exact solution of the wave equation,

$$\left( \nabla^2 - \frac{1}{c^2} \frac{\partial^2}{\partial t^2} \right) F(\mathbf{r}, t) = 0, \quad (4)$$

as follows:

$$F(\mathbf{r}, t) = \int dk g(k) e^{-ickt} \psi(\mathbf{r}; k), \quad (5)$$

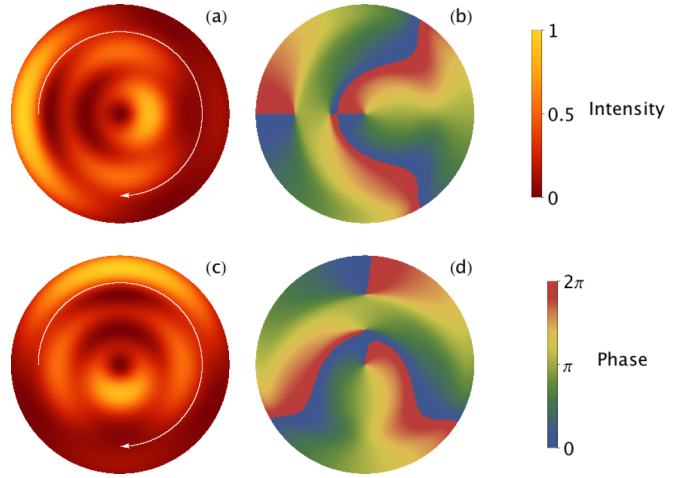


FIG. 2. Intensity and phase distribution for intensity rotating RSABs. Panels (a) and (c) correspond to the intensity distributions at  $z = 0$  and  $z = \pi/2\Omega$ , respectively, while panels (b) and (d) depict the corresponding phase profiles. The intensity and phase distributions have been plotted in the region  $0 < R < 1.5 \text{ mm}$ . The difference in plotting range with respect to Fig. 1 reflects the paraxial character of intensity rotating RSABs in contrast to the nonparaxial character of their field rotating counterparts. For these figures,  $\Omega = 75 \text{ rad/s}$ ,  $\lambda = 800 \text{ nm}$ ,  $\beta = 7.8 \mu\text{m}^{-1}$ , and  $C_m = 1$  for  $0 < m \leq 4$ , and  $C_m = 0$  otherwise, have been used. The white arrow in the intensity distribution shows the direction of rotation of the RSAB.

where  $g(k)$  is an arbitrary spectral function. If we then substitute into  $\psi(\mathbf{r}; k)$  the expression of a RSAB, as given by Eq. (3), we obtain the general expression for a radially self-accelerating pulse (RSAP), namely

$$F_{\text{RSAP}}(\mathbf{r}, t) = \sum_{m \in \mathcal{M}} C_m e^{im\Phi} \int dk g(k) e^{i(\beta z - ckt)} \times J_m[R\sqrt{k^2 - (m\Omega + \beta)^2}]. \quad (6)$$

Before proceeding any further, it is worth saying a few things about the general structure of the above integral. First of all, we can distinguish two different cases:  $\beta = 0$ , corresponding to field-rotating RSAPs, and  $\beta \neq 0$ , corresponding to intensity-rotating RSAPs. The latter case, however, can be further divided into two subclasses, namely the case  $\beta = \beta(k)$  [meaning that each monochromatic component of the RSAP defined in Eq. (6) will have its own global propagation constant], and the case  $\beta = \text{const} \neq 0$ . In the latter case, discussed below in Sec. II B, the spectrum of the RSAP is  $m$ -dependent, meaning that each component in the sum in Eq. (6) has to first be transformed into a polychromatic signal with its own spectrum, and then summed to form the RSAP. We will show that the case  $\beta = \beta(k)$  results in a pseudo-self-accelerating pulse, where self-acceleration is restored only asymptotically, while the case  $\beta = \text{const}$  will instead give rise to a rigorous, self-accelerating pulse.

#### A. Intensity-rotating RSAPs with $\beta = \beta(k)$

Let us first consider the case  $\beta = \beta(k) \neq 0$ . First we observe that, typically,  $\Omega \ll k$ , meaning that the rotation rate

of the RSAB is much smaller than its actual wave vector. If we substitute this ansatz into the argument of the Bessel function appearing in Eq. (6), we can Taylor-expand the square root appearing as an argument of the Bessel function in Eq. (6) with respect to the small parameter  $\Omega/k$ , thus obtaining

$$\sqrt{k^2 - (m\Omega + \beta)^2} \simeq k \left[ \sqrt{1 - \frac{\beta^2}{k^2}} - \frac{\beta}{\sqrt{k^2 - \beta^2}} \left( \frac{m\Omega}{k} \right) - \frac{km^2\Omega^2}{2(k^2 - \beta^2)^{3/2}} + O\left(\frac{\Omega^3}{k^3}\right) \right]. \quad (7)$$

Since  $\beta = \beta(k)$  can be chosen arbitrarily, we can assume, without loss of generality, that it can be written as  $\beta(k) = k \cos \xi$ , where  $0 < \xi < \pi/2$ . If we do so, we can simplify the expansion above as follows:

$$\sqrt{k^2 - (m\Omega + \beta)^2} \simeq k \sin \xi - m\Omega \cot \xi + O\left(\frac{\Omega^2}{k^2}\right), \quad (8)$$

or, by defining  $\Lambda = \Omega(\cos \xi / \sin^2 \xi)$  as the new angular velocity of the RSAP, we obtain

$$\sqrt{k^2 - (m\Omega + \beta)^2} \simeq \sin \xi (k - m\Lambda). \quad (9)$$

This approximation is valid provided that  $(m\Omega)/k \ll 1$ . Since the number of components of RSABs can be decided almost arbitrarily, however, it is possible to define a new set  $\mathcal{M}' = \{m \in \mathbb{N}_0 : m \ll (k/\Omega)\}$ , and therefore restrict the summation in Eq. (6) to the subset  $\mathcal{M}' \subset \mathcal{M}$ . If we do so, and introduce the change of variables  $k' = k - m\Lambda$ , we obtain a rather simple form for RSAPs, namely

$$F_{\text{RSAP}}^{(1)}(\mathbf{r}, t) = \sum_{m \in \mathcal{M}'} C_m e^{im\Theta_0} X_m(R, \zeta), \quad (10)$$

where  $\Theta_0 = \theta + \Lambda\zeta$  is the corotating coordinate, and

$$X_m^{(1)}(R, \zeta) = \int dk g(k) e^{ik\zeta} J_m(kR \sin \xi) \quad (11)$$

represents the general expression of an X-wave [23,24], with  $\zeta = z \cos \xi - ct$  being its correspondent comoving coordinate. This is the first result of our work. In the polychromatic domain, radially self-accelerating fields can be constructed by taking superpositions of X-waves rather than Bessel beams.

However, as can be seen from Eq. (10), intensity-rotating RSAPs intrinsically contain a  $\zeta$ -dependence on both their corotating coordinate  $\Theta_0$  and the transverse distribution  $X_m(R, \zeta)$ . This fact, which will be discussed in detail in the next section, is ultimately the reason why RSAPs only possess a pseudo-self-accelerating character.

At first glance, Eq. (11) has the same form of its monochromatic counterpart, namely Eq. (3), and could be interpreted as its straightforward generalization. One could in fact naively substitute Bessel beams, which are used in the monochromatic case to generate RSABs, with X-waves (i.e., polychromatic Bessel beams), thus realizing RSAPs.

A closer analysis of Eq. (10), however, reveals an important difference between the two cases, namely that while RSABs describe spiraling trajectories of constant transverse dimension [13], RSAPs describe spiraling trajectories of growing

transverse dimension. Moreover, while the transverse structure of RSABs rigidly rotates around the propagation axis, this is not the case for RSAPs, which instead show a progressive self-adaptation of the transverse intensity distribution to a ring, centered on the propagation axis.

To better understand this, let us consider explicitly the case of fundamental X-waves. These are characterized by an exponentially decaying spectrum, i.e.,  $g(k) = H(k) \exp[-\alpha k]$ , where  $\alpha$  accounts for the width of the spectrum, it has the dimensions of a length, and  $H(x)$  is the Heaviside step function. If we substitute this exponentially decaying spectrum into Eq. (10) and use Eq. 6.621.1 in Ref. [25], we get, after some simple algebraic manipulation, the following result:

$$F_{\text{RSAP}}^{(1)}(\mathbf{r}, t) = e^{i \arctan(\frac{\xi}{\alpha})} \sum_{m \in \mathcal{M}'} A_m e^{im\Theta} \frac{\rho^m}{\sqrt{\alpha^2 + \zeta^2}} {}_2F_1 \left( \frac{m+1}{2}, \frac{m+2}{2}; m+1; -\rho^2 e^{2i \arctan(\frac{\xi}{\alpha})} \right), \quad (12)$$

where

$$\rho \equiv \rho(\zeta) = \frac{R \sin \xi}{\sqrt{\alpha^2 + \zeta^2}} \quad (13)$$

is an expanding normalized radial coordinate,

$$\Theta = \theta + \Lambda\zeta + \arctan\left(\frac{\zeta}{\alpha}\right) \quad (14)$$

is the corotating, accelerating reference frame,  $A_m = C_m/2^m$ , and  ${}_2F_1(a, b; c; x)$  is the Gauss hypergeometric function [21]. Notice that although in general the hypergeometric function gives an extra  $m$ - and  $\zeta$ -dependent phase contribution, which modifies the definition of  $\Theta$ , if we limit ourselves to the case  $\xi \ll 1$ , the phase contribution of the hypergeometric function can, at leading order in  $\xi$ , be neglected.

We can now compare the two corotating coordinates in the monochromatic ( $\Phi$ ) and polychromatic ( $\Theta$ ) case: while  $\Phi$  essentially describes a helix centered around the  $z$ -axis, whose transverse width remains constant, since the angular velocity of the RSAB is  $\Lambda = \text{const}$ , this is not the case for the polychromatic corotating coordinate  $\Theta$ , as it represents an accelerating coordinate with velocity

$$\frac{\partial \Theta}{\partial \zeta} = \Lambda + \frac{\alpha}{\alpha^2 + \zeta^2} \quad (15)$$

and acceleration

$$\frac{\partial^2 \Theta}{\partial \zeta^2} = -\frac{2\alpha\zeta}{(\alpha^2 + \zeta^2)^2}. \quad (16)$$

The above expressions for the angular velocity and acceleration of the RSAP reveals that for large enough propagation distances,  $\partial \Theta / \partial \zeta \rightarrow \Lambda$  and  $\partial^2 \Theta / \partial \zeta^2 \rightarrow 0$ , and the standard values of velocity and acceleration for RSABs are restored. This means that the self-accelerating state represents an asymptotic equilibrium for the RSAP. For small propagation distances, on the other hand, the behavior of RSAPs changes significantly from traditionally self-accelerating beams, as can be seen from Eqs. (15) and (16). Since the corotating

coordinate is now accelerating, and the acceleration is toward the center of the pulse, the transverse field distribution needs to adapt to this attractive force, which tends (asymptotically) to transform the intensity distribution into a ring-shaped pulse around the comoving propagation direction  $\zeta$ . For these reasons, one cannot formally speak anymore of self-accelerating pulses, as there exists no reference frame in which Eq. (12) appears propagation-invariant, or, as said in other terms, there exists no reference frame in which the motion of the pulse around the  $\zeta$ -axis can be described by a helix. However, since the self-accelerating behavior is an asymptotical equilibrium of the system, one could refer to such pulses as pseudo-self-accelerating.

The intensity and phase distributions of intensity-rotating RSAPs are shown in Fig. 3. For small propagation distances [Figs. 3(a)–3(d)], the intensity distribution gets progressively distorted while propagating along  $\zeta$  up to the point at which the RSAP reaches its equilibrium form of a ring [Figs. 3(e) and 3(f)]. From this point on, the transverse intensity distribution does not change anymore in shape, but only becomes bigger due to the expanding nature of the radial comoving coordinate  $\rho$ , as can be seen by comparing panels (e) and (g) of Fig. 3. If we compare the behavior of RSAP at large  $\zeta$  with that of RSABs, we can notice that while the transverse dimension of the spiral described by RSABs remains constant (essentially because  $\Phi$  describes a helix rather than a spiral), this is not the case for RSAPs, since  $\Theta$  describes a spiral, whose transverse dimension is growing with  $\zeta$ .

To estimate this, let us calculate the average transverse size of the spiral, by considering the position of the center of mass of the RSAP intensity distribution, as follows:

$$\langle R(\zeta) \rangle = \int d^2R R |F_{\text{RSAP}}(\mathbf{r}, t)|^2 \equiv R_0 \sqrt{\alpha^2 + \zeta^2}, \quad (17)$$

where, at the leading order in  $\xi$  [26],

$$R_0 = \frac{2\pi}{\sin^3 \xi} \sum_{m \in \mathcal{M}'} |A_m|^2 \int_0^\infty d\rho \rho^{2(m+1)}, \quad (18)$$

Thus, in the comoving, expanding, reference frame, the transverse dimension of the spiral grows as  $\sqrt{\alpha^2 + \zeta^2}$ .

### B. Intensity-rotating RSAPs with $\beta = \text{const}$

Another possibility for intensity-rotating RSAPs is to choose  $\beta = \text{const} \neq 0$ . If we use this assumption, introducing the change of variables  $k' = \sqrt{k^2 - (m\Omega + \beta)^2}$  in Eq. (6), and if we allow the spectral function  $g(k)$  to be  $m$ -dependent and redefine it as  $g_m(k) = (2kG_m(k)/\sqrt{k^2 - (m\Omega + \beta)^2})H(k)$ , where  $H(k)$  is the Heaviside step function [21], we get the following result:

$$F_{\text{RSAP}}^{(2)}(\mathbf{r}, t) = e^{i\beta z} \sum_{m \in \mathcal{M}'} C_m e^{im\Phi} X_m^{(2)}(R, t; \beta), \quad (19)$$

where

$$X_m^{(2)}(\mathbf{r}; \beta) = \int_0^\infty dk G_m(k) e^{-ictA(k)} J_m(kR), \quad (20)$$

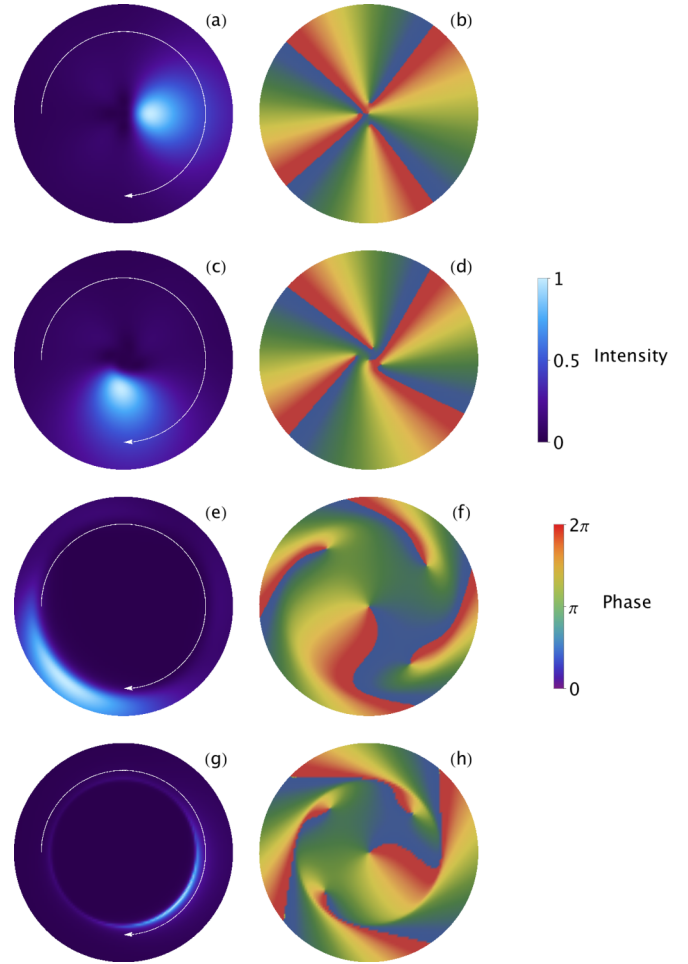


FIG. 3. Intensity (left) and phase (right) distribution for intensity-rotating RSAPs, as defined by Eq. (12). The plots are made at different values of the normalized propagation length  $\zeta \equiv \zeta/\alpha$ , namely  $\zeta = 0$  [panels (a) and (b)],  $\zeta = 2\pi/\Lambda$  [panels (c) and (d)],  $\zeta = 10(2\pi/\Lambda)$  [panels (e) and (f)], and  $\zeta = 50(2\pi/\Lambda)$  [panels (g) and (h)]. As can be seen, the transverse profile of intensity-rotating RSAPs gets progressively distorted, up to the point at which it stabilizes in a ring-shaped form [panel (e)]. The intensity and phase distributions have been plotted in the region  $0 < \rho < 1250$  for panels (a)–(f), and  $0 < \rho < 7500$  for panels (g) and (h). For these figures,  $\Omega = 75$  rad/s,  $\lambda = 800$  nm,  $\xi = 0.01$  (corresponding to  $\beta = 7.853 \times 10^6$  m $^{-1}$ ), and  $C_m = 1$  for  $1 < m \leq 4$ , and  $C_m = 0$  otherwise, have been used. The white arrow in the intensity distribution shows the direction of rotation of the RSAP.

where  $A(k) = \sqrt{k^2 + (m\Omega + \beta)^2}$ . If we choose the spectral function  $G(k)$  as

$$G(k) = \frac{1}{\sqrt{k^2 + (m\Omega + \beta)^2}}, \quad (21)$$

Eq. (20) admits the following closed-form analytical solution [25]:

$$X_m^{(2)}(R, t; \beta) = I_{m/2} \left[ \frac{\alpha}{2} (\sqrt{R^2 - c^2 t^2} - ict) \right] \times K_{m/2} \left[ \frac{\alpha}{2} (\sqrt{R^2 - c^2 t^2} + ict) \right], \quad (22)$$



where  $I_m(x)$  and  $K_m(x)$  are the modified Bessel function of the first and second kind, respectively [21], and  $\alpha = m\Omega + \beta$ .

As can be seen, no  $z$ -dependence is contained in the expression of the transverse field distribution  $X_m^{(2)}(R, t; \beta)$ , and Eq. (19) has the same form of Eq. (3). In this case, therefore, we can define the corotating reference frame  $\{R, \Phi, t\}$ , where  $F_{\text{RSAP}}^{(2)}(\mathbf{r}, t)$  is manifestly propagation-invariant. However, due to the presence of the modified Bessel function of the second kind,  $K_{m/2}(x)$ , this field distribution is divergent in the origin, and therefore it cannot represent a physically meaningful solution. Analytical forms of intensity-rotating RSAPs, therefore, only exist for  $\beta = \beta(k)$ . This is the second result of our work: intensity-rotating RSAPs can only be constructed by assigning a proper  $\beta(k)$  to each of the monochromatic components that contribute to the pulse. If  $\beta$  is constant, no physically meaningful analytical solution can be found.

Notice, however, that a trivial possibility for describing intensity-rotating RSAPs with constant  $\beta$  would be to consider the case  $\beta = \text{const} \ll 1$ . This, however, can be treated (at least at leading order in  $\beta$ ) as a first-order correction to the case  $\beta = 0$ , which will be discussed in the next section. Since  $\beta = 0$  will correspond to field-rotating RSAPs, one could then conclude that intensity-rotating RSAPs with constant small  $\beta$  can be well described by field-rotating RSAPs.

### C. Field-rotating RSAPs

For the case  $\beta = 0$ , the argument for the Bessel function in Eq. (6) becomes  $\sqrt{k^2 + m^2\Omega^2}$ . If we then assume that  $\Omega \ll k$ , and use the expansion in Eq. (7) with  $\beta = 0$  up to  $O(\Omega^2/k^2)$ , we can write  $\sqrt{k^2 - m^2\Omega^2} \simeq k$ . This approximation, however, holds as long as  $m$  is chosen in such a way that  $m\Omega/k \ll 1$ . As stated before, since we are free to choose the set in which  $m$  is defined, we can restrict the original set  $\mathcal{M}$  to the new subset  $\mathcal{M}' \equiv \{m \in \mathbb{N}_0 : m \ll (\sqrt{2}k/\Omega)\}$ . In this case, the explicit expression of field-rotating RSAPs is given as follows:

$$F_{\text{RSAP}}^{(3)}(\mathbf{r}, t) = \sum_{m \in \mathcal{M}'} C_m e^{im\Phi} X_m^{(3)}(R, \zeta_0), \quad (23)$$

where  $\zeta_0 = -ct$ , and

$$X_m^{(3)}(R, \zeta_0) = \int dk g(k) e^{ik\zeta_0} J_m(kR). \quad (24)$$

Notice that unlike the case  $\beta \neq 0$ , no  $z$ -dependence is present in the transverse form of the pulse  $X_m^{(3)}(R, \zeta_0)$ . This means that field-rotating RSAPs are truly self-accelerating fields, as one can define a reference frame, namely  $\{R, \Phi, \zeta_0\} \equiv \{R, \Phi, t\}$ , in which the RSAP appears propagation-invariant, and fulfills all the required conditions for self-acceleration [13]. The intensity and phase distributions for field-rotating RSAPs at different propagation lengths are shown in Fig. 4. As it can be seen, the transverse intensity profile remains unchanged as the pulse propagates along  $z$ . Notice, moreover, that field-rotating RSAPs rotate in the opposite direction with respect to intensity-rotating RSAPs.

## IV. CONCLUSIONS

In this work, we have generalized the concept of radially self-accelerating field to the domain of optical pulses. We have

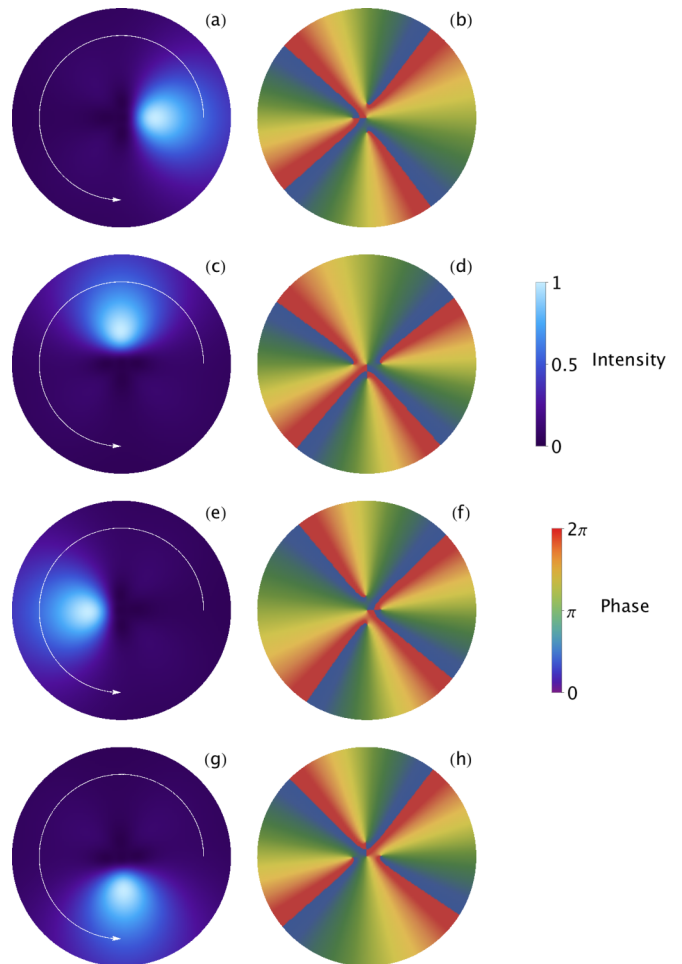


FIG. 4. Intensity (left) and phase (right) distribution for field-rotating RSAPs at different values of the propagation length, namely  $\zeta = 0$  [panels (a) and (b)],  $\zeta = 0.25(2\pi/\Lambda)$  [panels (c) and (d)],  $\zeta = 0.5(2\pi/\Lambda)$  [panels (e) and (f)], and  $\zeta = 0.75(2\pi/\Lambda)$  [panels (g) and (h)]. As can be seen, the transverse profile of field-rotating RSAPs remains propagation-invariant, and rotates synchronously with its phase profile. The intensity and phase distributions have been plotted in the region  $0 < R < 10 \mu\text{m}$ . For these figures,  $\Omega = 75 \text{ rad/s}$ ,  $\lambda = 800 \text{ nm}$ , and  $C_m = 1$  for  $1 < m \leq 4$ , and  $C_m = 0$  otherwise, have been used. The white arrow in the intensity distribution shows the direction of rotation of the RSAP.

shown how it is possible to define RSAPs as a superposition of OAM-carrying X-waves, rather than Bessel beams. For the case of fundamental X-waves, we have calculated the explicit expression for field-rotating, as well as intensity-rotating, RSAPs, and we have shown that while the former retain their self-acceleration character, the latter possess pseudo-self-acceleration and admit pure self-acceleration only asymptotically. We have also investigated intensity-rotating RSAPs with constant  $\beta$ , and we showed that although in this case it is possible to recover pure self-acceleration, such fields have no physical meaning, as they are divergent in the origin. Our work represents an attempt to generalize the concept of self-acceleration to the domain of optical pulses, and it discusses advantages and limitations of this process. Moreover, our work represents a guideline that will be useful for the

experimental realization of radially self-accelerating optical pulses.

In future works, we intend to investigate the properties of RSAPs under focusing, and compare them with their monochromatic counterparts [27], to see if the introduction of polarization as an extra degree of freedom can balance the occurrence of pseudo-self-acceleration. In addition, we will also investigate the quantum properties of both RSABs

and RSABs in terms of their linear and angular momentum content, as well as their nonlinear interaction with matter [28].

#### ACKNOWLEDGMENT

The authors wish to thank the Deutsche Forschungsgemeinschaft (Grant No. SZ 276/17-1) for financial support.

- 
- [1] M. V. Berry and N. L. Balazs, *Am. J. Phys.* **47**, 274 (1979).
- [2] G. A. Siviloglou, J. Broky, A. Dogariu, and D. N. Christodoulides, *Phys. Rev. Lett.* **99**, 213901 (2007).
- [3] G. A. Siviloglou and D. N. Christodoulides, *Opt. Lett.* **32**, 979 (2007).
- [4] Y. Hu, G. A. Siviloglou, P. Zhang, N. K. Efremidis, D. N. Christodoulides, and Z. Chen, *Self-accelerating Airy Beams: Generation, Control, and Applications in Nonlinear Photonics and Novel Optical Phenomena* (Springer, Berlin, 2012).
- [5] J. Baumgartl, M. Mazilu, and K. Dholakia, *Nat. Photon.* **2**, 675 (2008).
- [6] P. Polynkin, M. Kolesik, J. V. Moloney, G. A. Siviloglou, and D. N. Christodoulides, *Science* **324**, 229 (2009).
- [7] M. A. Bandres, *Opt. Lett.* **33**, 1678 (2008).
- [8] M. A. Bandres, *New J. Phys.* **15**, 013054 (2013).
- [9] M. A. Bandres, M. A. Alonso, I. Kaminer, and M. Segev, *Opt. Express* **21**, 13917 (2013).
- [10] M. A. Bandres, *Opt. Lett.* **34**, 3791 (2009).
- [11] I. Kaminer, R. Bekenstein, J. Nemirovsky, and M. Segev, *Phys. Rev. Lett.* **108**, 163901 (2012).
- [12] J. Zhao, I. D. Chremmos, D. Song, D. N. Christodoulides, N. K. Efremidis, and Z. Chen, *Sci. Rep.* **5**, 12086 (2015).
- [13] C. Vetter, T. Eichelkraut, M. Ornigotti, and A. Szameit, *Phys. Rev. Lett.* **113**, 183901 (2014).
- [14] C. Vetter, T. Eichelkraut, M. Ornigotti, and A. Szameit, *Appl. Phys. Lett.* **107**, 211104 (2015).
- [15] J. Webster, C. Rosales-Guzman, and A. Forbes, *Opt. Lett.* **42**, 675 (2017).
- [16] C. Vetter, A. Dudley, A. Szameit, and A. Forbes, *Opt. Express* **25**, 20530 (2017).
- [17] A. Jesacher and M. J. Booth, *Opt. Express* **18**, 21090 (2010).
- [18] A. Mathis, L. Froehly, L. Furfaro, M. Jacquot, J. M. Dudley, and F. Courvoisier, *J. Eur. Opt. Soc.: Rapid Publ.* **8**, 13019 (2013).
- [19] D. McGloin, V. Garces-Chavez, and K. Dholakia, *Opt. Lett.* **28**, 657 (2003).
- [20] S. Sukhov and A. Dogariu, *Opt. Lett.* **35**, 3847 (2010).
- [21] F. W. J. Olver, D. W. Lozier, R. F. Boisvert, and C. W. Clark, *NIST Handbook of Mathematical Functions* (Cambridge University Press, Cambridge, 2010).
- [22] J. Durnin, J. J. Miceli, and J. H. Eberly, *Phys. Rev. Lett.* **58**, 1499 (1987).
- [23] *Localized Waves*, edited by H. E. Hernandez-Figueroa, M. Zamboni-Rached, and E. Recami (Wiley, Hoboken, NJ, 2008).
- [24] M. Ornigotti, C. Conti, and A. Szameit, *Phys. Rev. Lett.* **115**, 100401 (2015).
- [25] I. S. Gradshteyn and I. M. Ryzhik, *Table of Integrals, Series and Products* (Academic, Cambridge, MA, 2006).
- [26] Please note that the integral in the definition of  $R_0$  in Eq. (18) diverges. This, however, is only due to the particular choice of spectrum  $g(k)$ , which leads to infinite-energy-carrying X-waves. For a more realistic and experimentally realizable case, a Gaussian profile for  $g(k)$  can be chosen, which corresponds to a finite radial integral in the definition of  $R_0$ .
- [27] M. Ornigotti and A. Szameit, *J. Opt.* **20**, 125601 (2018).
- [28] M. Ornigotti and A. Szameit (unpublished).